RSC Advances

COMMUNICATION

Cite this: *RSC Adv.*, 2015, **5**, 27393

Dissolution of upconverting fluoride nanoparticles in aqueous suspensions†

D. Lisjak,*[a] O. Plohl,[ab] M. Ponikvar-Svet[a] and B. Majaron[a]

Received 15th January 2015
Accepted 12th March 2015

DOI: 10.1039/c5ra00902b

www.rsc.org/advances

The chemical stability of upconverting, lanthanide-doped, fluoride nanoparticles in aqueous media, which shows great potential in bio-imaging, was studied. The partial dissolution of selected nanoparticles ($NaYF_4$, LaF_3 and GdF_3) co-doped with Yb^{3+} and Tm^{3+} was detected and compared with respect to their size, chemical composition and structure.

Fluorescent, lanthanide-doped nanoparticles (Ln-NPs) have recently received a lot of interest due to their potential applications in biomedicine; especially in bioimaging, but also in therapy.[1–3] The fluorescence of the Ln-NPs is an intrinsic property of the Ln ions, which distinguishes them from quantum dots and Au NPs, in which the fluorescence originates from size-related effects (quantum confinement and surface plasmon resonance, respectively).[4]

Consequently, Ln-NPs of any size can, in principle, absorb and emit near-infrared (NIR) light with significantly deeper penetration, reduced tissue damage and negligible auto-fluorescence, in comparison to the excitation with visible or ultraviolet light. For this reason Ln-NPs, featuring a NIR-to-NIR upconversion (UC), have been intensively studied. The UC process is characterized by the emission of light with shorter wavelengths than that of the excitation source. In particular, NPs co-doped with Yb^{3+} and Tm^{3+} can be excited *via* the absorption by Yb^{3+} of NIR light with around 980 nm followed by energy transfer to the excited states of Tm^{3+}, which can be relaxed by emitting NIR (around 800 nm) or blue light.[1] In addition to the dopant concentrations, the efficiency of the UC fluorescence also depends on the matrix of the host crystal. Due to their lower phonon energy and, consequently, lower, nonradiative losses, fluoride matrices are preferred over the oxides.[1,2]

Various binary (LnF_3, Ln = Sc, Y, La–Lu) and ternary fluoride matrices ($MLnF_4$, M = Li, Na, K) Ln-NPs were studied previously.[3,5,6] Different methods were proposed for the synthesis of Ln-NPs with controlled size, morphology, stability in different solvents, and optimized UC efficiency. While solvothermal (including hydrothermal) syntheses can be designed to produce hydrophilic Ln-NPs, as well as being ecofriendly and suitable for scaling-up, thermal decomposition in high-boiling-point solvents yields Ln-NPs with a better crystallinity, a more homogenous size and superior UC properties.[1,7] In the latter case, the hydrophobic surfaces of the as-synthesized UC-NPs need to be modified into hydrophilic surfaces for *in vivo* applications. The application of the Ln-NPs in biomedical imaging and therapy was proposed based on their presumed low toxicity.[5,8] However, despite the known chemical stability and poor solubility (*i.e.*, chemical solubility and not colloidal stability, which is often denoted as solubility) of bulk Ln-fluorides[9,10] a partial dissolution of selected Ln-NPs in water was observed in this study. NPs often show higher solubility rates with respect to coarser particles or bulk material, since the solubility rate depends on the surface-area-to-volume ratio, the surface roughness and the curvature.[11] Namely, smaller particles with a smaller radius of positive curvature are energetically unfavourable and their equilibrium solubility is larger than that of coarser particles.

In accordance with the above, larger solubilities were determined for the binary Ln-fluoride (LnF_3) powders than for the respective single crystals.[12] The solubility products of LnF_3 powders in water at 25 °C are low and increase with the increasing atomic number of the Ln: from $K_{sp} = 3.26 \times 10^{-21}$ for LaF_3 powders to $K_{sp} = 1.26 \times 10^{-19}$ for LuF_3 powders, with a significantly higher solubility of ScF_3, $K_{sp} = 2.98 \times 10^{-12}$.[10] For comparison, the solubility product of water-soluble NaF is $K_{sp} = 7.1 \times 10^{-1}$.[12] The solubility also depends on the pH and can be also additionally altered by the presence of other ions or ligands, which can form soluble complexes with Ln^{3+} or F^-.[13,14] Consequently, the solubility

[a]*Jožef Stefan Institute, Jamova 39, SI-1000 Ljubljana, Slovenia. E-mail: darja.lisjak@ijs.si*

[b]*Jožef Stefan International Postgraduate School, Jamova 39, SI-1000 Ljubljana, Slovenia*

† Electronic supplementary information (ESI) available: Details of experimental procedure: synthesis and characterization and XRD diffractograms of the as-synthesized Ln-NPs. See DOI: 10.1039/c5ra00902b

of the NPs is also affected by the synthesis conditions. Ion leakage and dissociation at the surface of the NPs represents another possibility for the release of potentially toxic ions.[11]

The solubility data for ternary Ln-fluorides are very limited, as they are considered to be stable and not hygroscopic.[1,2,9] Nevertheless, a relatively high solubility ($K_{sp} = 2.55 \times 10^{-12}$) was reported for NH_4ScF_4.[15] The leakage of Ln^{3+} from UC-NPs (for example, in $NaYF_4$, CaF_2, and Gd_2O_3 matrices) and their (cyto)toxicity was questioned before.[16] A limited number of studies report on the genesis of nephrogenic systemic fibrosis and calcific uremic arteriolopathy induced by the released Gd^{3+} from Gd-based MRI contrasting agents and on the neurotic symptoms caused by La^{3+} and Yb^{3+}.[17] It is also demonstrated that sufficiently large concentrations (around few mM) of F^- (and HF, which is present at pH < 3) present a cytotoxic threat in different tissues.[18] The apoptosis and/or necrosis were caused by the F^- *in vitro* and *in vivo* due to the induction of inflammatory reactions, cell contraction, the inhibition of protein synthesis, cell-cycle progression, oxidative stress and/or DNA damage. Therefore, a systematic solubility analysis of the fluoride Ln-NPs is necessary for an evaluation of their potential cytotoxic effect.

In this work we present, for the first time, data on the dissolution of selected binary and ternary fluoride Ln-NPs: LaF_3, GdF_3, and $NaYF_4$ co-doped with Yb^{3+} and Tm^{3+}. The Ln-NPs with sizes of 10–100 nm were synthesized in aqueous and non-aqueous media. The dissolution of Ln-NPs in water suspensions was detected in all the samples, regardless of their size, structure and the synthesis method.

Ln-NPs with compositions of $NaYF_4$, LaF_3 and GdF_3 co-doped with Yb^{3+} (20 at%) and Tm^{3+} (2 at%) were synthesized hydrothermally (HT), solvothermally (ST) or with thermal decomposition (TD) using established procedures.[7,19] The samples were denoted as listed in Table 1. The detailed experimental procedures are given in the Experimental section in the ESI.†

The X-ray diffraction (XRD) analysis (Fig. S1 in ESI†) suggests that all the samples are single phase. NaY-HT and NaY-ST NPs both crystallized in a cubic, α-$NaYF_4$, structure, while hexagonal, β-$NaYF_4$, NPs were synthesized with the TD method. La-HT and La-ST NPs crystallized in a hexagonal structure, and Gd-HT and Gd-ST NPs crystallized in an orthorhombic structure. For all the compositions Ln-NPs with smaller sizes were obtained with the ST synthesis than with the HT synthesis, while their crystal structures were the same for both synthesis methods (Table 1).

Transmission electron microscope (TEM) images (Fig. 1) show the difference in morphology between the different Ln-NPs. The NaY-ST sample consists of a mixture of spherical and anisotropic (elongated) Ln-NPs, while the NaY-TD and NaY-HT (not shown) NPs are (nearly) spherical. The La-HT and Gd-HT are of irregular and anisotropic shape, and the aggregates of the Gd-HT NPs have similar shapes to the individual Ln-NPs. These specific shapes of the binary HT samples are similar to their ST counterparts, *i.e.*, La-ST and Gd-ST. The selected-area electron diffraction of all the samples confirmed the structures identified with the XRD analyses and the energy-dispersive X-ray spectroscopy analysis confirmed the presence of all the constituent elements, including a minor fraction of O. The latter could originate from the surface ligands (CA, PEI or OA; see Experimental section in ESI†).

The UC fluorescence spectra of the NaY-NPs (Fig. 2) show most prominent emission in the NIR, around 800 nm. Six individual transitions were identified within this emission band, with peaks at 770, 782, 793, 800, 817, and ~834 nm. This matches the potential for 6-fold splitting of the Tm^{3+} ground state manifold, $^3H_6$. The spectral structure of this emission provides a valuable insight into the interaction of the Tm^{3+}

Table 1 Basic properties and the dissolution data of the Ln-fluoride NPs

Sample name	Crystal structure	Ln-NPs size (nm)	Dissolved ions per formula unit (mol%)
NaY-HT	α-$NaYF_4$	103 ± 10	F: 0.99 ± 0.02
			Na: 5.61 ± 0.03
			Y: 0.20 ± 0.01
			Yb: 0.21 ± 0.01
			Tm: 0.34 ± 0.01
NaY-ST	α-$NaYF_4$	20 ± 3 (spherical)	F: 1.05 ± 0.03
			Na: 5.97 ± 0.02
		(45 ± 12) × (22 ± 5) (elongated)	Y: 0.46 ± 0.01
			Yb: 0.46 ± 0.01
			Tm: 0.83 ± 0.13
NaY-TD	β-$NaYF_4$	21 ± 3	F: 0.39 ± 0.11
			Na: 2.33 ± 0.1
			Y: 0.08 ± 0.01
			Yb: 0.10 ± 0.01
			Tm: 0.20 ± 0.05
La-HT	Hexagonal LaF_3	20 ± 5	F: 0.65 ± 0.01
La-ST	Hexagonal LaF_3	13 ± 3	F: 1.16 ± 0.05
Gd-HT	Orthorhomb. GdF_3	(63 ± 17) × (36 ± 10)	F: 0.30 ± 0.01
Gd-ST	Orthorhomb. GdF_3	(48 ± 15) × (24 ± 7)	F: 0.30 ± 0.02

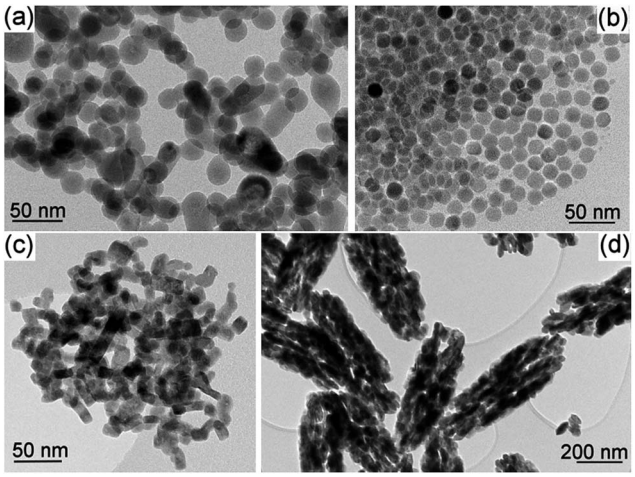

Fig. 1 TEM images of the as-synthesized nanoparticles: (a) NaY-ST, (b) NaY-TD, (c) La-HT and (d) Gd-HT.

electronic levels involved in the respective radiative transition (*i.e.*, $^3H_4 \rightarrow {}^3H_6$) with the local crystal field. *E.g.*, the broadening of individual emission peaks in NaY-ST, as compared to NaY-HT, indicates a more disordered crystal matrix. This is in agreement with the considerably smaller size of the latter NPs (Table 1) and their broader XRD peaks (see Fig. S1 in the ESI†). In the NaY-TD NPs, in contrast, only 3 transitions are evident in the same spectral range, with the 800 nm peak dominating over those at 782 and 817 nm (Fig. 2, bottom). In addition, the UC emission is considerably stronger than in the HT- and ST-samples, in agreement with earlier reports.[1,9] (Note that a factor of 3 was applied in Fig. 2 to reveal the structure of the first two spectra.) This reflects the difference in crystal structure (between α-$NaYF_4$ and β-$NaYF_4$; see Table 1), as revealed also by XRD. The UC fluorescence in blue (peaks at 448 and 474 nm) was much weaker in comparison to the NIR emission, as already reported before.[20] Faint UC emission of Tm^{3+} was observed also around 540, 643, 658, and 695 nm. The small peaks at 582/592 nm can be attributed to impurities originating from the reagents.

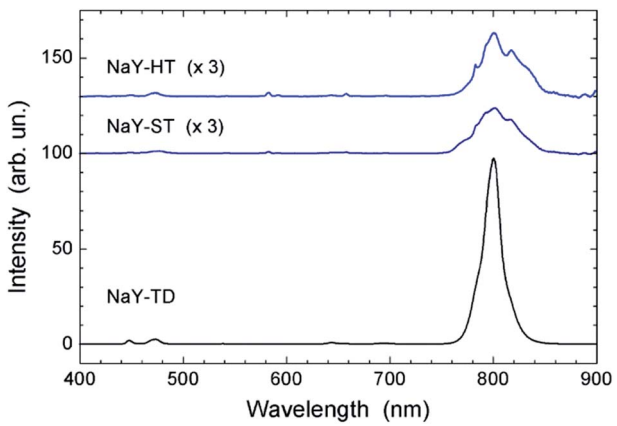

Fig. 2 UC fluorescence spectra of the NaY-NPs in aqueous suspensions. In order to make the weak fluorescence of the HT- and ST-samples perceptible, their spectra were multiplied by a factor of 3.

The dissolution of the fluoride Ln-NPs was analysed with an Orion 960 Autochemistry System using a combined fluoride ion selective electrode for a potentiometric determination of the F^- using the multiple known addition method with a blank subtraction[21] while the concentration of dissolved cations (Ln^{3+}, Y^{3+} and Na^+) was determined using an optical emission spectrometer with inductively coupled plasma. For details see the Experimental section in the ESI.† The F^- was detected in aqueous suspensions of all the investigated Ln-NPs.

In the following we compare the dissolution of the fluoride Ln-NPs with respect to the synthesis method/medium, matrix structure and composition, and particle size (Fig. 3):

(1) Synthesis medium: no general difference was observed between the Ln-NPs synthesized in aqueous (HT) and non-aqueous (ST and TD) environments if samples of the same composition are considered. A lower dissolution was measured for the La-HT than for the La-ST NPs, but the latter were considerably smaller (see point 4). Meanwhile, the significantly lower dissolution of the NaY-TD in comparison with the NaY-HT and NaY-ST NPs can be attributed primarily to the difference in the crystal structure (see point 2).

(2) Matrix crystal structure: ternary Ln-NPs with a metastable cubic crystal structure (α-$NaYF_4$: NaY-HT and NaY-ST) showed a significantly higher solubility than those with a thermodynamically stable hexagonal phase (β-$NaYF_4$: NaY-TD).

(3) Matrix composition: the Gd-NPs showed the lowest dissolution of F^- among all the samples, while the highest dissolution degree was detected for metastable α-$NaYF_4$ NPs and 10 nm-sized La-ST NPs. The dissolution degree of the β-$NaYF_4$ NPs was comparable to those of the Gd-NPs.

(4) Ln-NPs size: no significant effect of the Ln-NPs size on the dissolution of F^- was observed. Only in the case of the La-NPs was a higher dissolution degree measured for the smaller La-HT than for the larger La-ST NPs.

Although no general effect of the above-discussed parameters on the dissolution of fluoride Ln-NPs was observed, we can conclude, without any doubt, that the superior chemical stability of the NaY-TD NPs can be attributed to their thermodynamically stable, hexagonal structure (β-$NaYF_4$) in comparison to the NaY-ST and NaY-HT NPs with a metastable cubic structure (α-$NaYF_4$). This was further supported by the

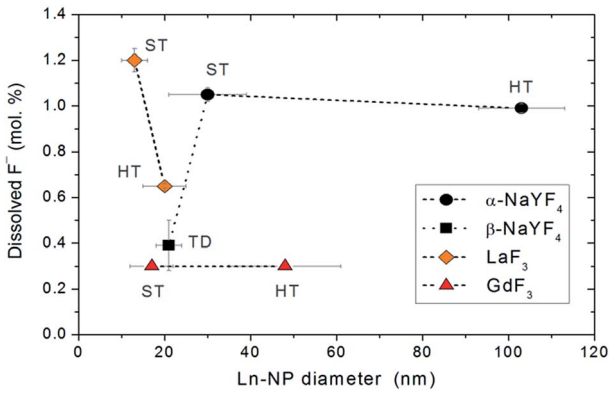

Fig. 3 Comparison of the dissolution degree of Ln-NPs.

dissolution analysis of the other constituent ions in these samples. The concentrations of dissolved cations varied in a similar way to those of F^- (Table 1), again suggesting a superior stability of the NaY-TD NPs. The concentration of dissolved F^- (per formula unit) was higher than that of the Ln^{3+}, while the concentration of the dissolved Na^+ was by far the highest. A similar trend was observed before in binary fluorides,[13] while in ternary fluorides only the dissolution of Ln^{3+} ions was analyzed.[16] The stoichiometrically excessive solubility of the F^- in comparison to the Ln^{3+} ions can be a consequence of the different dissolution processes: (1) the dissolved Ln^{3+} ions form stable insoluble complex(es) with ligands (Lig) present in water, like, for example, –OH or dissolved capping agents (CA, PEI), while the F^- remains dissolved:

$$NaLnF_4(s) \xleftrightarrow{H_2O} Na^+ + Ln^{3+} + 3F^- \quad (1a)$$

$$Ln^{3+} + n\ Lig(aq) \xleftrightarrow{H_2O} Ln - Lig_n(s) \quad (1b)$$

(2) The deficient F^- ions are substituted by the dissolved ligands, *i.e.*, O^{2-}, –OH:

$$NaLnF_4(s) \xleftrightarrow{H_2O} NaLn - F_{4-x}{}^{+x}(s) + x\ F^- \quad (2a)$$

$$NaLn - F_{4-x}{}^{+x}(s) + x\ Lig(aq) \xleftrightarrow{H_2O} NPs - Ln - (Lig)_x(s) \quad (2b)$$

(3) The dissolution only affects the surface layer, which is typically chemically and structurally defected in comparison to the core of the particle. Therefore it would be possible for the Ln-NPs surface layer to have an excess of F^-.

An even higher degree of the dissolution per formula unit was detected for the Na^+ (Table 1). This can be partly explained in a similar way as for the F^-. Other possible source for the excessive Na^+ can originate from an inadequate purification step, during which the excess of Na^+ from the synthesis may not be completely eliminated. It would also be possible for the dissolution of the surface $NaYF_4$ layer to be accompanied by a transformation into YF_3:

$$NaLnF_4(s) \xleftrightarrow{H_2O} LnF_3(s) + Na^+ + F^- \quad (3)$$

This explanation can be correlated with the lowest measured relative concentration of Y^{3+}.

A comprehensive additional study, beyond the scope of this work, is in progress to elucidate the dissolution mechanism of the fluoride Ln-NPs. Nevertheless, the dissolved ions may have a toxic effect on the cells. Here, the F^- seems more problematic due to its higher solubility than that of Ln^{3+}. For example, the concentration of F^- in aqueous suspensions with 1 mg ml^{-1} of Ln-NPs having an α-$NaYF_4$ structure is around 0.2 mM (Table 1). When the *in vivo* local concentration of the Ln-NPs exceeds 5 mg ml^{-1}, the concentration of the free F^- would be high enough to induce cell death by different mechanisms[18] (see above). In addition to this, in the acidic media (pH < 3.18), like, for example, in lysosomes, the dissolved fluorine species is HF with $pK_a = 3.18$,[22] which is even more toxic than F^-:

$$HF + H_2O \leftrightarrow H_3O^+ + F^- \quad (4)$$

Although Gd-NPs appear more stable and thus would be preferable for biomedical applications, binary fluorides, in general, suffer from a poorer UC fluorescence efficiency[1,8] than can be achieved in the $NaYF_4$ matrix. Therefore, among the studied fluoride Ln-NPs, the most suitable ones would be NaY-TD NPs with a β-$NaYF_4$ structure, which show superior chemical stability and UC fluorescent properties (Fig. 2).

Conclusions

Despite the known chemical stability and poor solubility of bulk Ln-based fluorides, this is not entirely true in the case of nanoparticles. The partial dissolution of Ln-based, fluoride, upconverting nanoparticles ($NaYF_4$, LaF_3 and GdF_3 co-doped with Yb^{3+} and Tm^{3+}) was detected. Between 0.2 and 1.1 mol% of F^- was dissolved in the suspension of nanoparticles with a concentration of 1 mg ml^{-1}, while the fraction of the dissolved Ln^{3+} was between 0.2 and 0.8 mol%. The GdF_3 and β-$NaYF_4$ nanoparticles were more stable in comparison to the others. However, binary fluorides, in general, suffer from a poorer UC fluorescence efficiency[1,8] than can be achieved in the $NaYF_4$ matrix. The chemical stability of the ternary Ln-based fluoride nanoparticles coincides with the thermodynamic stability of their crystal structures since the dissolution degree of the β-$NaYF_4$ nanoparticles was significantly lower than that of the α-$NaYF_4$. Considering the great potential of UC $NaYF_4$: Yb, Tm nanoparticles in biomedicine, their dissolution in water and the potential cytotoxic effects should be studied in more detail.

Acknowledgements

The work was financially supported by Slovenian Research Agency within the Research Programs P2-0089 and P1-0045. The authors acknowledge the use of equipment in Center of Excellence in Nanosciences and Nanotechnology. The authors also thank Dr Alenka Mertelj for assistance with optical setup.

Notes and references

1 F. Wang and X. Liu, *Chem. Soc. Rev.*, 2009, **38**, 976.
2 A. Gnach and A. Bednarkiewicz, *Nano Today*, 2012, **7**, 532.
3 L. Cheng, C. Wang and Z. Liu, *Nanoscale*, 2013, **5**, 23.
4 L. M. Maestro, E. M. Rodriquez, F. Vetrone, R. Naccache, H. L. Ramirez, D. Jaque, J. A. Capobianco and J. G. Sole, *Opt. Express*, 2010, **18**, 23544.
5 W. Feng, X. Zhu and F. Li, *NPG Asia Mater.*, 2013, **5**, e75.
6 C. X. Li, J. Yang, P. P. Yang, H. Z. Lian and J. Lin, *Chem. Mater.*, 2008, **20**, 4317; F. Wang, Y. Han, C. S. Lim, Y. Lu, J. Wang, J. Xu, H. Chen, C. Zhang, M. Hing and X. Liu, *Nature*, 2010, **463**, 1061; D. Yang, G. Li, X. Kang, Z. Cheng, P. Ma, C. Peng, H. Lian, C. Li and J. Lin, *Nanoscale*, 2012, **4**, 3450.

7 F. Ventrone, R. Naccache, A. Zamarron, A. J. dela Fuente, F. Sanz-Rodriguez, L. M. Maestro, E. M. Rdoriguez, D. Jaque, J. G. Sole and J. A. Capobianco, *ACS Nano*, 2010, **4**, 3254; C. Li, Z. Quan, J. Yang, P. Yang and J. Lin, *Inorg. Chem.*, 2007, **46**, 6329; H. S. Qian and Y. Zhang, *Langmuir*, 2008, **24**, 12123.

8 A. Xia, M. Chen, Y. Gao, D. Wu, W. Feng and F. Li, *Biomaterials*, 2012, **33**, 5394; Q. Xiao, Y. Li, F. Li, M. Zhang, Z. Zhang and H. Lin, *Nanoscale*, 2014, **6**, 10179.

9 J. Ganem, J. Crawford, P. Scmidt, N. W. Jenkins and S. R. Bowman, *Phys. Rev. B: Condens. Matter Mater. Phys.*, 2002, **66**, 245101.

10 H. Itoh, H. Hachiya, M. Tsuchiya, Y. Suzuki and Y. Asano, *Bull. Chem. Soc. Jpn.*, 1984, **57**, 1689.

11 Y. M. Chiang and W. D. Kingery, *Physical Ceramics*, John Wiley & Sons, Inc., 1997, p. 351; P. Borm, F. C. Klaessig, T. D. Landry, B. Moudgil, J. Pauluhn, K. Thomas, R. Trottier and S. Wood, *Toxicol. Sci.*, 2006, **90**, 23.

12 D. Wu, X. Wu, Y. Lu and H. Wang, *Mater. Lett.*, 2008, **62**, 3003.

13 T. Mioduski, C. Guminski and D. Zheng, *J. Phys. Chem. Ref. Data*, 2014, **43**, 013105.

14 D. Rai, M. Yu, A. Kitamura, H. Yoshikawa and A. R. Felmy, *J. Solution Chem.*, 2013, **42**, 1500.

15 Y. V. Sokolova and R. N. Cherepanin, *Russ. J. Appl. Chem.*, 2011, **84**, 1319.

16 E. Hemmer, T. Yamano, H. Kishimoto, N. Venkatachalam, H. Hyod and K. Soga, *Acta Biomater.*, 2013, **9**, 4734; Y. F. Wang, L. D. Sun, J. W. Xiao, W. Feng, J. C. Zhou, J. Shen and C. H. Yan, *Chem.–Eur. J.*, 2012, **18**, 5558.

17 T. Grobner, *Nephrol., Dial., Transplant.*, 2006, **21**, 1104; L. Amuluru, W. High, K. M. Hiatt, J. Ranville, S. V. Shar, B. Malik and S. Swaminathan, *J. Am. Acad. Dermatol.*, 2009, **61**, 73; D. R. Broome, *Eur. J. Radiol.*, 2008, **66**, 230; L. X. Feng, H. Q. Xiao, X. He, Z. J. Li, F. L. Li, N. Q. Liu, Y. L. Zhao, Y. Y. Huang, Z. Y. Zhang and Z. F. Chai, *Toxicol. Lett.*, 2006, **165**, 112; H. Q. Xiao, F. L. Li, Z. Y. Zhang, L. X. Feng, Z. J. Li, J. H. Yang and Z. F. Chai, *Toxicol. Lett.*, 2005, **155**, 247.

18 N. I. Agalakova and G. P. Gusev, *ISRN Cell Biol.*, 2012, 403835; O. Babier, L. Arreola-Mendoza and L. M. Del Razo, *Chem.-Biol. Interact.*, 2010, **188**, 319.

19 N. Bogdan, F. Vetrone, G. A. Ozin and J. A. Capobianco, *Nano Lett.*, 2011, **11**, 835; C. X. Li, J. Yang, P. P. Yang, H. Z. Lian and J. Lin, *Chem. Mater.*, 2008, **20**, 4317; X. Qu, K. Y. Yang, J. W. Chung, B. K. Moon, B. C. Choi, J. H. Jeong and K. H. Kim, *J. Solid State Chem.*, 2011, **184**, 246.

20 G. Chen, T. Y. Ohulchanskyy, R. Kumar, H. Ågren and P. N. Prasad, *ACS Nano*, 2010, **4**, 3163.

21 M. Ponikvar, V. Stibilj and B. Žemva, *Food Chem.*, 2007, **103**, 369.

22 G. T. Hefter, *J. Solution Chem.*, 1984, **13**, 457.